

# Prototype of a system with coordinated operation of an electrolyzer for load stability in solar-powered hydrogen production

Salas-Flores, J.1  Velarde-Allazo, E.2 

<sup>1</sup>Universidad Tecnológica del Peru, Peru, u18211989@utp.edu.pe

<sup>2</sup>Universidad Tecnológica del Peru, Peru, evelarde@utp.edu.pe

**Abstract**– *The following work evaluates the stability of solar energy for use as an energy source in a system that can provide AC and DC voltage for the production and storage of green hydrogen. For electrolysis, a conventional alkaline electrolyzer (AEL) is used, and in the first section, the optimal concentration of potassium hydroxide (KOH) will be defined to avoid oversaturating the concentration. The following sections consist of recording the charge captured by the solar panels, the efficiency of the PWM and MPPT controllers, in addition to seeing the stability provided by the two systems and the amount of hydrogen produced with the charge obtained.*

**Keywords** – *Green hydrogen, electrolysis, solar energy, electrolyzer, power stabilization, MPPT controller*

## I. INTRODUCTION

Solar and wind energy are not stable sources of energy, whether due to wind intensity, weather changes, or even the presence of a bird. This variability (voltage drops, voltage spikes, ramps, low-load operations) is the primary cause of electrolysis system degradation.

Water electrolysis for hydrogen production using solar energy is a promising technology, but it faces challenges that depend on weather, the movement of the sun, or other factors that alter the charge. [1] In this case, a system is sought that can compensate for all these failures and provide stable energy 24 hours a day, autonomously.

Electrolyzers that can be AEL or with proton exchange membrane (PEME) are exposed to losing their capacity due to the degradation of their electrodes, a product of the charge instability of their energy source. [2]

Hydrogen production powered by solar energy is a major step toward decarbonizing traditional energy sources, promoting this type of clean energy, and providing a means of long-term energy storage.

Hydrogen is produced by different methods, some of which can generate greenhouse gas emissions, of these, 75% is produced with natural gas, 23% with coal and only 2% by electrolysis. Among these alternatives, the most promising is electrolysis,

since it only requires electricity and water as inputs, therefore, it has a high potential to generate green hydrogen, that is, production with low or zero emissions. Production depends on the solar energy source. In their study, the economic and environmental benefits of the combination of renewable energy supply and the electricity grid for water electrolysis were analyzed. [3]

The implemented system will use clean, free energy sources such as solar radiation; however, an implementation cost will be considered, which requires periodic maintenance and cleaning. This type of work fosters industrial innovation and reduces dependence on external sources. [4]

According to the diagram in Figure 1, the system will focus on 4 stages: collection, adaptation, storage and production.

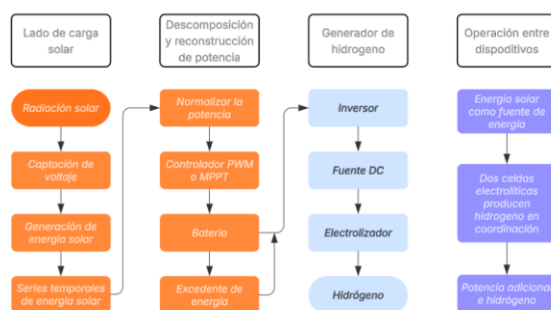


Figure 1: Flow diagram of the stabilizer system.

From the stages shown, the energy entering the panels and the energy exiting through the inverter and the load dedicated to storage will be quantified, according to Figure 2.

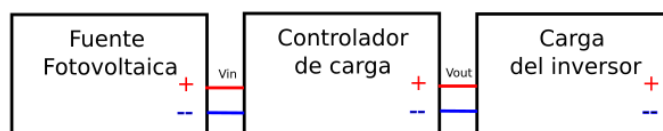


Figure 2: DC load diagram.

## II. METHODS AND MATERIALS

### A. Methodology for producing hydrogen and oxygen by electrolysis.

This process will be carried out with the module represented in figure 1. This has a hydrogen conduit that is connected to 2 pipettes with a scale where the reaction occurs in a container with pure water.

After the reaction, the 2 pipettes will store 20 ml of gas at ambient atmospheric pressure.

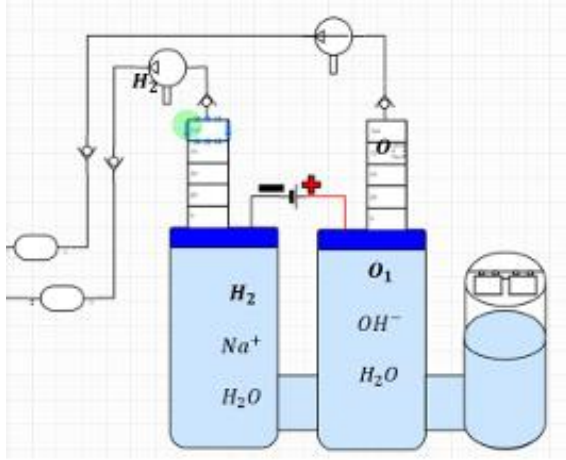
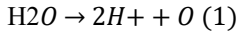
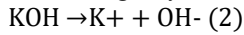


Figure 3: water electrolysis scheme.

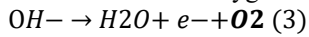
To obtain hydrogen, water must dissociate from its compound form when subjected to an electric current.



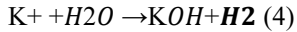
Potassium Hydroxide when dissolved in water dissociates in the following way



The OH is attracted to the positive pole and this will release an excess electron and oxygen is released.



In the same way, the K<sup>+</sup> cation, when attracted to the negative pole, will collect electrons that the negative pole will give it, the cation reacts immediately with water as indicated in the following equation.



The dissociation of K<sup>+</sup> ions and OH<sup>-</sup> ions in aqueous solutions provides a high density of free ions which makes it conduct electric current. [5] The atomic mass of hydrogen (H = 1.0797 g/mol then we can say:

1mol of H<sub>2</sub> a 1 atm = 1.0079 With a density of 0.071g/ml.

By carrying out the reaction 4 times we obtain the following overall reaction of the system  $2H_2O \rightarrow 2H_2 + O_2$

2mol of H<sub>2</sub> a 1 atm = 2.0158g.

To measure the flow rate of hydrogen, a graduated cylinder connected to a pipe that sends hydrogen was used. The volume of hydrogen occupied in the cylinder and the time it takes to occupy this space were measured.

$$Q = V_{H_2} \text{ mL/t} \quad (5)$$

Table 1: Hydrogen production time

N°	KOH (Mol)	Voltaje (V)	Corriente (A)	Tiempo
1	1.16	18.8	0.75	00:05:38
2	2.38	18.8	1.23	00:02:50
3	3.57	18.8	2.54	00:01:43
4	4.76	18.8	3.58	00:00:40
5	5.95	18.8	5.01	00:00:20
6	7.14	18.8	5.51	00:00:20
7	8.33	18.8	6.01	00:00:20
8	9.52	18.8	6.55	00:00:21

With the data recorded in table 1, the graph in figure 4 is generated.

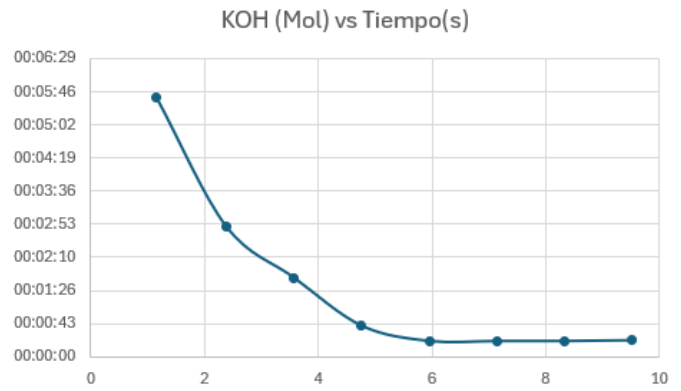


Figure 4: Hydrogen production by KOH concentration.

The graph seeks to identify the relationship between KOH concentration and hydrogen production and to identify how the system is affected by this. [6]

In the electrodes there is the anode that is connected to the positive part of the power supply, in this electrode oxygen will be produced, on the contrary, the cathode that is connected to the negative will produce hydrogen, which would be the main fuel for the FC. The materials commonly used for the electrodes are platinum, iridium, or nickel due to their corrosion resistance and good conductivity. Stainless steel electrodes can also be used, preferably good quality 304 or 316, or stainless steel covered with nickel or platinum, which are those materials where the highest performance and duration of the electrodes were obtained [7].

To calculate this you can use Faraday's law, using this formula you can calculate the hydrogen separated from the water considering the amount of current consumed by the electrolyzer, using formula 6.

$$W = \frac{I * T * M}{n * F} \quad (6)$$

The technologies that predominate in the electrolysis process are alkaline electrolysis, proton exchange membrane electrolysis, and solid oxide electrolysis. These offer

advantages and problems that must be evaluated for their implementation.[8]

The alkaline electrolyzer is the most established technology due to its low cost and long lifespan. On the other hand, there is the proton exchange membrane electrolyzer, which is more efficient but requires electrodes composed of precious metals as a catalytic agent. Although they can further increase their efficiency by operating at high temperatures, their deterioration is also accelerated.[9]

The alkaline electrolyte electrolyzer is low-cost to manufacture due to inexpensive catalysts such as nickel and stainless steel, and has a long lifespan. However, it presents challenges such as a larger operating size compared to the other methods mentioned. Therefore, this technology is the most mature and has undergone more studies on its operation and the environmental impact of producing hydrogen.[10]

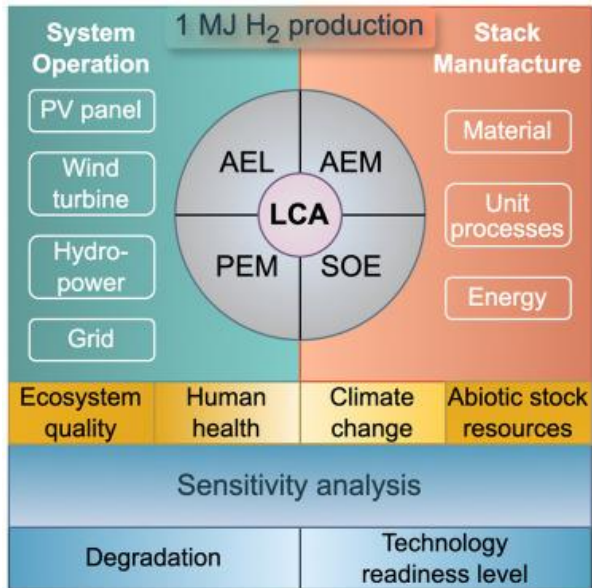


Figure 5: Graphic summary of the types of hydrogen production [10]

With the information gathered, it was decided on an electrolyzer with alkaline electrolyte, which is shown in figure 6.

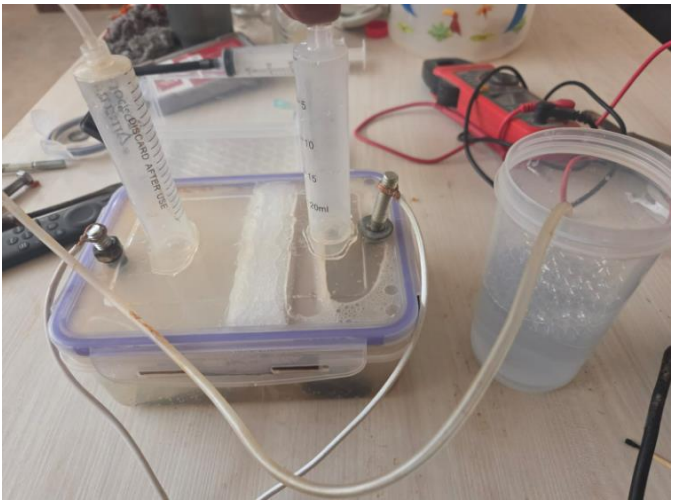


Figure 6: prototype electrolyzer.



Figure 7: 12V diaphragm pump for gas collection.  
To demonstrate that hydrogen gas is pure, the gas produced was extracted through a controlled nozzle, which is seen in Figure 8. In this experiment, the gas flame remains constant and does not produce an explosion, since it only encounters oxygen when leaving the nozzle.

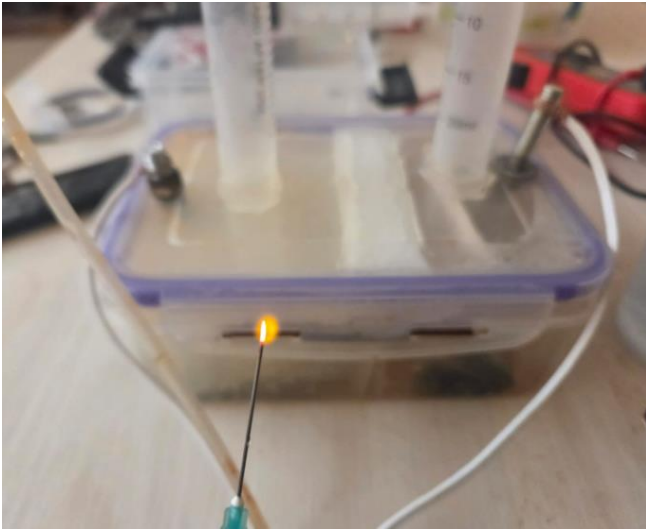


Figure 8: Combustion of hydrogen gas produced by the alkaline electrolyzer.

The atmospheric pressure of Arequipa according to the Meteostat meteorological database is shown in Figure 9 and this pressure is 1027hPa or 102.7KPa, in addition the temperature is approximately 15.3°C and the recorded volume of the gas was 20ml.

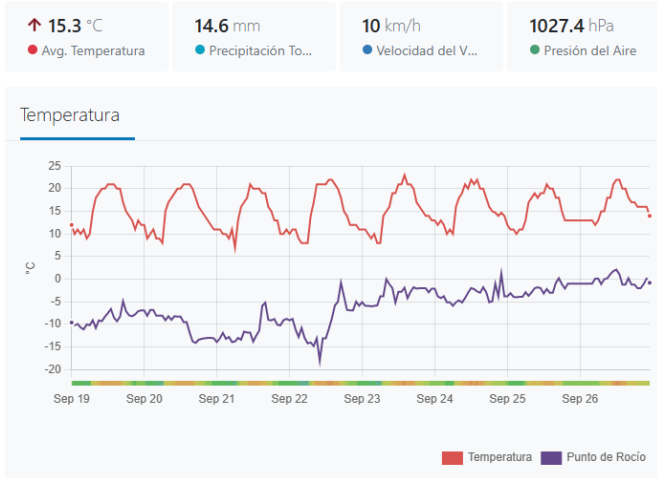


Figure 9: Meteorological data for Arequipa.

With the data available, the values are normalized to the ideal gas formula, which is more than sufficient for mass calculations:  $V=0.02$  L,  $P=1.0136$  atm,  $T=288.15$  °K,  $R=0.082057$  L.atm/(mol.°K), and  $M=2.016$  g/mol.

$$n = \frac{P \cdot V}{R \cdot T} \quad (7)$$

$$n = 1.0136 \cdot \frac{0.020}{0.082057 \cdot 288.15} \text{ mol} \quad (8)$$

$$n = 8.57 \times 10^{-4} \text{ mol} \quad (9)$$

To normalize the result, moles are converted to grams.

$$m = n \cdot M \quad (10)$$

$$m = 8.57 \cdot 10^{-4} \cdot 2.016 \text{ g} \quad (11)$$

$$m = 1.7 \text{ mg } H_2 \quad (12)$$

So now we have two pieces of data: the electrolyzer's hydrogen production is 1.7 mg every 20 seconds with a constant power consumption of 94 watts. If we want to produce 1 kg of hydrogen, we would have to calculate it using equation 13.

$$1 \text{ Kg} = N^\circ \text{ ciclos} \cdot 1.7 \text{ mg} \quad (13)$$

$$N^\circ \text{ ciclos} = \frac{1000g}{0.0017g} = 588235.29 \approx 588235 \text{ ciclos} \quad (14)$$

Each cycle takes 20 seconds, so equation 15 is used to obtain the total time it takes to produce 1 kg of hydrogen, then the value is normalized to hours using equation 16.

$$t(s) = 588235 \cdot 20s = 11,764,705 \text{ s} \quad (15)$$

$$t(h) = \frac{11,764,705 \text{ s}}{60s \cdot \frac{60min}{h}} = 3,268 \text{ horas} \quad (16)$$

Now that we have the time it takes to produce 1 kg of hydrogen in hours, the kWh needed to produce this amount is calculated with equation 17 and to obtain the total energy needed, the energy conversion efficiency obtained by the solar panels is considered, which is 86.78%.

$$\text{Consumo de energía} = 3,268 \text{ h} \cdot 94W = 307 \text{ kWh} \quad (17)$$

$$\text{Consumo Total} = \frac{307 \text{ kWh}}{0.8678} = 353 \text{ kWh} \quad (18)$$

The results obtained by KS Hayibo can be appreciated, which are shown in Figure 10, where he manages to produce 1 kg of hydrogen with 74.45 kWh with an efficiency of 71% in a 5 kW plant. In this case, it can be seen that his electrolyzer cell with an anion exchange membrane is much more efficient than the electrolyzer used in this work, since the energy consumption of the proposed prototype is 4.74 or almost 5 times higher than that proposed by Hayibo.

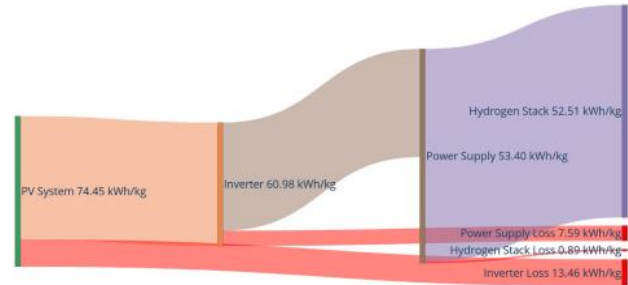


Figure 10: Average energy loss diagram for producing 1 kg of hydrogen using an FPV-AEM system [12]

### B. System data collection with PWM load control.

For the collection of solar energy data and its adaptation, a provisional prototype with a PWM controller was implemented, which can be seen in Figure 11.



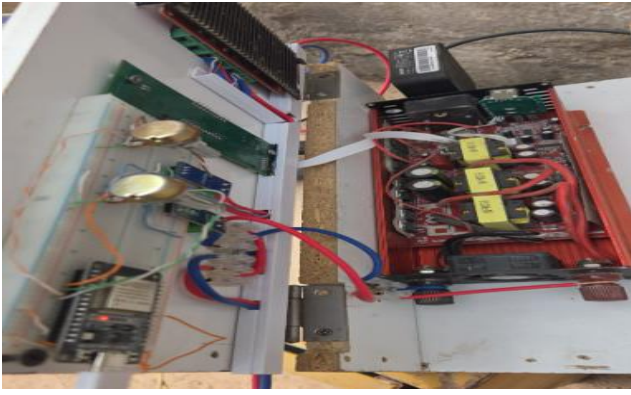


Figure 11: Solar energy stabilizer assembly.

Using an ESP32 as a data acquisition interface, the charging behavior of a 185W panel with 36 Vmp and 5.15 Imp was recorded. This data is shown in Figure 12, which graphs the voltage recorded every 2 minutes.

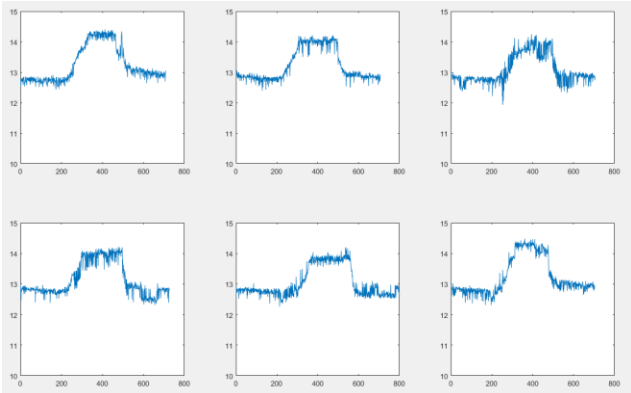


Figure 12: Sampling charging voltage over a full day with a PWM controller

Figure 13 shows the charging current performance, which starts at 7:30 a.m., the current increases until the battery is fully charged at 11:30 a.m., and that is when the PWM controller cuts off the current and prevents the battery from being overcharged and deteriorated.

Being a PWM controller, the control is on-off, so a current that oscillates from 0 to 4.5 amps is displayed the rest of the day.

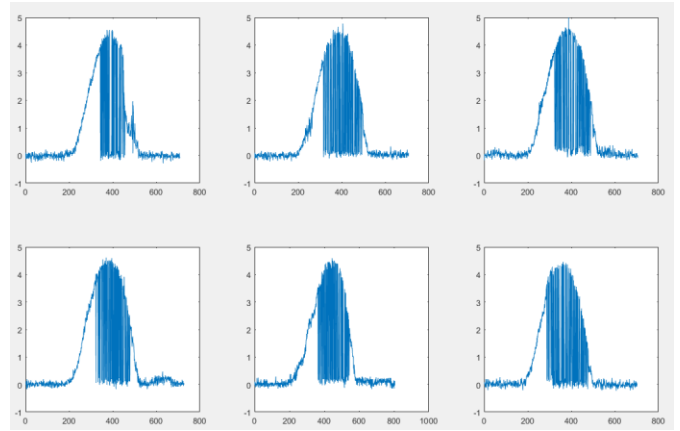


Figure 13: Current entering the battery with a PWM controller.

### III. ANALYSIS AND RESULTS

#### A. Solar load analysis with the PWM controller.

With the data obtained from the instantaneous voltages and currents, the instantaneous power of each sample can be obtained and by making a cumulative sum of these data, the Wh produced in a day of no-load operation can be obtained, which is graphed in Figure 14.

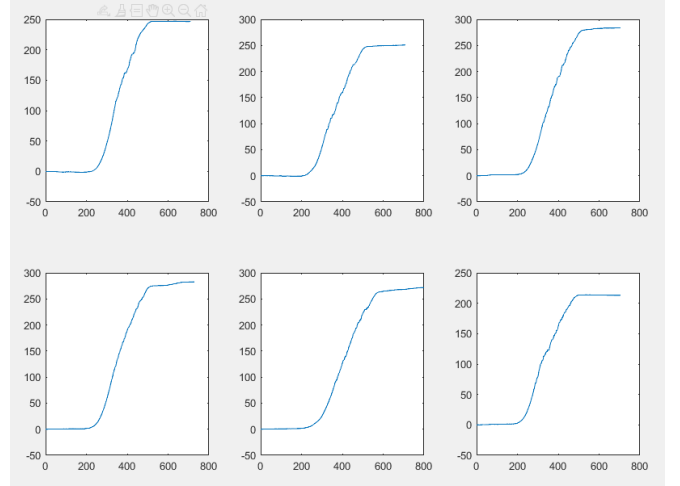


Figure 14: Cumulative power of solar energy in one day.

Table 2: Cumulative power in Wh

Sample	Cumulative power (Wh)
1	32.24 Wh
2	392.7 Wh
3	473.8 Wh
4	471.2 Wh
5	312.8 Wh
6	494 Wh
<b>362.79 Wh</b>	

In this case, it is indicated that it is 362.79 Wh and if we consider that in the field experience an AGM battery was used and it must be charged 112% to replenish its full charge.

$$Panel\ solar\ Wh = \left( \frac{Pot(electrolizador) * 24\ Wh}{+Pot(Bateria)\ Wh} \right) * 112\% \quad (19)$$

$$362.79\ Wh = \left( \frac{Pot(electrolizador) * 24h}{+12.7V * Ah(bateria)} \right) * 112\% \quad (20)$$

The experiment used a 150 Ah battery, the electrolyzer used consumed 94 W, and the battery charge must reach 112% of its capacity. According to equation 20, the system must receive photovoltaic charge for 10 hours according to the recorded periods. According to equation 24, the system requires a 500 W solar source.

$$PV * 10\ h = (94W * 24\ h + 12.7V * 150Ah) * 112\% \quad (21)$$

$$PV * 10\ h = (2256\ Wh + 1950Wh) * 112\% \quad (22)$$

$$PV = 4710.72 \frac{Wh}{10h} = 471\ W \quad (23)$$

$$PV \approx 500\ W \quad (24)$$

#### C. System data collection with MPPT charge control.

With the same data acquisition device, the voltages of the solar panel and the battery could be recorded, these can be seen in figure 15, the voltage of the panel is blue and that of the battery is orange,

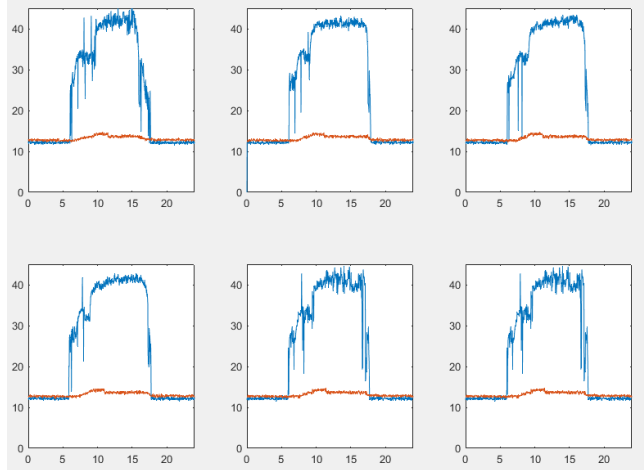


Figure 15: Solar panel and battery voltage.

Using the same method, the charging current was recorded in 6 scenarios, which are graphed in Figure 16. In the graph, the orange curve represents the current provided by the solar panel, and the blue curve is the output current transformed and adapted by the controller.

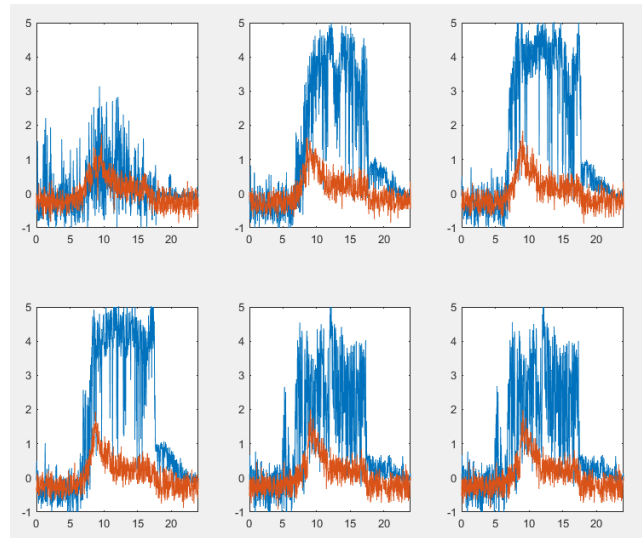


Figure 16: Input and output current of the MPPT controller.

According to Figure 17, the new 150W panel configuration ranges from 20 to 25 volts (V), and the battery voltage is replenished from 9V to 14.4V which is the maximum charge of an AGM battery.

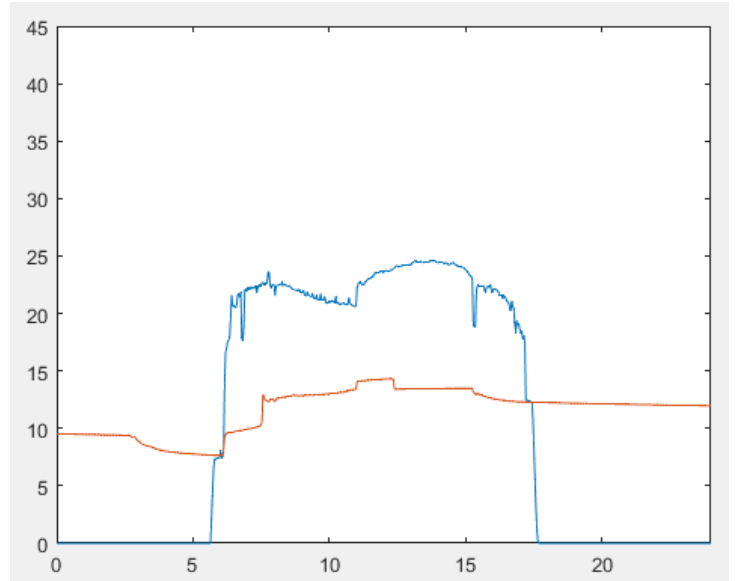


Figure 17: Solar panel and battery voltage.

#### B. Solar load analysis with the MPPT controller.

The recorded data is noisy and difficult to visualize, so an exponential moving average filter is applied, which averages the incoming values, but gives more weight to recent entries than to older ones. In this case, formula 25 was applied and with this, figure 18 is graphed.

$$Y(s) = \alpha * y(s) + (1 - \alpha) * Y(s - 1) \quad (25)$$

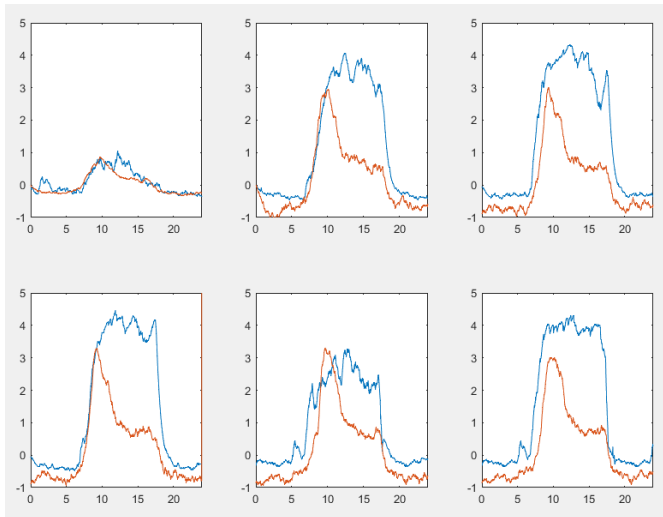


Figure 18: Input and output current graph of the MPPT controller

Considering the voltage and current values of the MPPT controller, statistical values of the MPPT controller are obtained, which are shown in Table 5.

Table 3: MPPT controller analysis.

Sample	I <sub>saw</sub> prom	I <sub>o</sub> prom	V <sub>o</sub> prom	I <sub>o</sub> prom	V <sub>o</sub> var
1	17.693	0.015	13.148	0.090	0.275
2	18.939	0.171	13.145	1.177	0.296
3	18.672	0.107	13.166	1.431	0.295
4	18.761	0.191	13.149	1.423	0.294
5	18.181	0.164	13.153	0.947	0.298
6	18.264	0.209	13.138	1.503	0.275
	18.419	0.143	13.150	1.095	0.289

Taking the statistical values of the recorded data, it is shown that the average voltage of the PWM controller is 0.2 V higher than that of the MPPT controller, however, the average current of the MPPT controller is higher by 295 mA.

With the data collected and graphed in Figure 19, the accumulated input and output power of the control system could be calculated. To evaluate the efficiency of the system, 6 representative samples were taken and from these the efficiency of the system will be averaged.

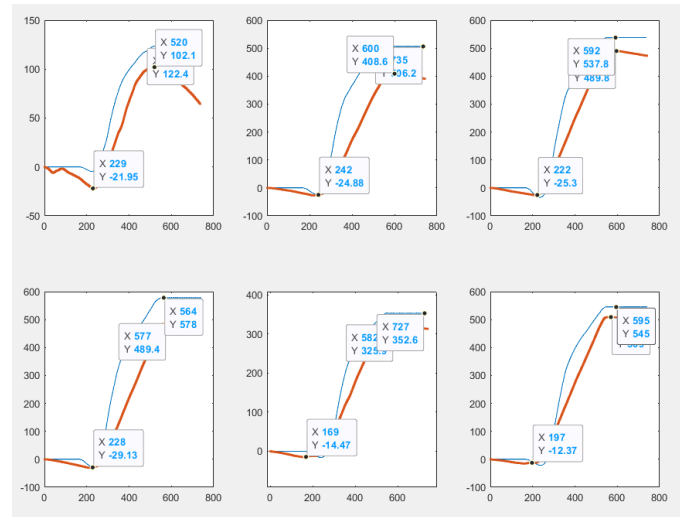


Figure 19: Cumulative power of the system.

From the curves recorded in figure 22, the maximum and minimum points are taken to quantify the total Wh of the 6 cases, this data is placed in table 7 and making a percentage calculation it is defined that the output power is 86.78% of the captured solar power.

Table 4: Charging efficiency

Sample	Maximum load point	Wh of the solar panel	Maximum controller output point	Wh of the controller	System efficiency
1	122.4	127.5	102.1	107.2	84.08%
2	506.2	8	408.6	433.48	81.62%
3	592	617.3	489.8	515.1	83.44%
4	578	3	489.4	518.53	85.41%
5	352.6	7	325.5	339.97	92.62%
6	545	7	509	521.37	93.54%
				average	86.78%

### C. System data analysis with MPPT charge control with a 150W, 26V panel.

The study demonstrates the feasibility of integrating solar photovoltaic energy with an AEM electrolyzer for hydrogen production. The results show energy efficiency ranging from 73.3% to 86.2%.[12]

By implementing the same control system in a 150W panel with 26 voltage at maximum power ( $V_{mp}$ ) and 5.7 Imp, the load performance was recorded in 24 hours and the accumulated energy is shown in the graph in figure 20, and obtained a total efficiency of 86.75%, which is similar to the average obtained in table 7.

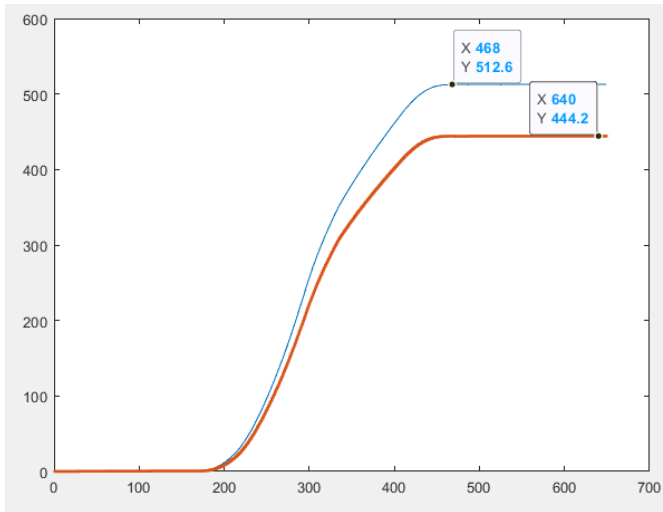


Figure 20: Cumulative system power with a 150 W panel.

#### IV. CONCLUSIONS

The work defined that the optimal molar concentration for electrolysis is 6 molar, since a lower amount reduces hydrogen production and a higher amount generates greater energy consumption and does not increase the production of the desired gas.

The 185-watt solar panel was able to provide the necessary power to support the autonomous operation of the electrolyzer system and allows for the addition of two additional electrolyzers that handle the same capacity.

A prototype has been implemented that controls the solar panel charge and records the system's input and output power. It also stores it on a microSD card and sends it to a Google Drive sheet. A system was implemented that quantifies the hydrogen produced by counting cycles, in addition to being able to quantify the efficiency of the system.

The system's efficiency reached 86.78%, thus fulfilling the null hypothesis proposed in the research. However, the electrolyzer's energy consumption produces little more than a fifth of the hydrogen gas produced by Hayabi due to the type of electrolyzer used and its design.

The possibility of integrating photovoltaic panels and alkaline electrolyzers on a larger scale opens up opportunities for optimizing off-grid solar photovoltaic systems, especially in a region like Arequipa, where solar radiation is highest and excess energy remains underutilized.

The coordinated electrolysis system with a solar energy source is a safe and functional prototype for completing the proposed experiment. The gas extraction method successfully separates the gases, but it cannot bring the electrodes closer together without compromising the mixing or fusion of one gas with another.

#### V. RECOMMENDATIONS

It is important to maintain a constant electrolyte concentration, otherwise hydrogen production is reduced or the energy may produce heat.

The solar panel does not reach its maximum performance even if the panel is directed normally toward the sun, but the power increases after a cloudy day.

It's important to include a scheduled restart in your code, as external failures can cause the system to lose communication and have trouble sending data to the cloud.

It is important to implement a filter or loop that averages the measured values, since otherwise the captured signal is usually very noisy.

Despite the potential of the electrolyzer system with a photovoltaic energy source, the system has limitations such as variations in solar radiation and overproduction without excessive battery storage.

The inefficiency of energy conversion, especially from direct current to alternating current and vice versa, since these electrolyzers are devices that operate solely on direct current, could be powered directly from solar panels, but the conversion efficiency is low and the voltage instability is very high, making a direct connection unsuitable.

#### REFERENCES

- [1] Z. Bai *et al.*, "Enhancing flexibility in wind-powered hydrogen production systems through coordinated electrolyzer operation," *Advances in Applied Energy*, p. 100228, Jun. 2025, doi: 10.1016/j.adapen.2025.100228.
- [2] A. Al-Douri, S. Wismer, A. Jimenez, and KM Groth, "Quantitative risk assessment of a lab-scale hydrogen electrolyzer system," *J Loss Prev Process Ind*, vol. 97, Oct. 2025, doi: 10.1016/j.jlp.2025.105680.
- [3] H. Ameli, D. Pudjianto, G. Strbac, and NP Brandon, "The impact of hydrogen on decarbonization and resilience in integrated energy systems," *Advances in Applied Energy*, vol. 17, Mar. 2025, doi: 10.1016/j.adapen.2024.100200.
- [4] I. Staffell *et al.*, "The role of hydrogen and fuel cells in the global energy system," Feb. 01, 2019, Royal Society of Chemistry. doi:10.1039/c8ee01157e.
- [5] Y. Zuo *et al.*, "High-performance alkaline water electrolyzers based on Ru-perturbed Cu nanoplatelets cathode," *Nat Commun*, vol. 14, no. 1, p. 4680, Aug. 2023, doi: 10.1038/s41467-023-40319-5.
- [6] Y. Guo, P. Qi, Q. Zhang, M. Li, J. Liu, and H. Sun, "Control strategy for hydrogen production system using HTO-based hybrid electrolyzers," *Energy Reports*, vol. 13, pp. 2354–2364, Jun. 2025, doi: 10.1016/j.egy.2025.01.012.
- [7] X. Zhang, M. Schwarze, R. Schömäcker, R. van de Krol, and FF Abdi, "Life cycle net energy assessment of sustainable H<sub>2</sub> production and hydrogenation of chemicals in a coupled photoelectrochemical device," *Nat Commun*, vol. 14, no. 1, p. 991, Feb. 2023, doi: 10.1038/s41467-023-36574-1.
- [8] A. Franco and C. Giovannini, "Recent and Future Advances in Water Electrolysis for Green Hydrogen Generation: Critical Analysis and Perspectives," *Sustainability*, vol. 15, no. 24, p. 16917, Dec. 2023, doi: 10.3390/su152416917.
- [9] Y. Astriani, W. Tushar, and M. Nadarajah, "Optimal planning of renewable energy park for green hydrogen production using detailed cost and efficiency curves of PEM electrolyzer," *Int J Hydrogen Energy*, vol. 79, pp. 1331–1346, Aug. 2024, doi: 10.1016/j.ijhydene.2024.07.107.
- [10] X. wei *et al.*, "Comparative life cycle analysis of electrolyzer technologies for hydrogen production: Manufacturing and operations," *Joule*, vol. 8, no. 12, pp. 3347–3372, Dec. 2024, doi: 10.1016/j.joule.2024.09.007.
- [11] J. Wang, L. Kang, and Y. Liu, "Optimal design of a renewable hydrogen production system by coordinating multiple PV arrays and multiple electrolyzers," *Renew Energy*, vol. 225, May 2024, doi: 10.1016/j.renene.2024.120304.
- [12] KS Hayibo, G. Antonini, MM Rahman, and JM Pearce, "Experimental integration of a foam-based floating photovoltaic (floatovoltaic)



system with an anion exchange membrane electrolyzer for 5 kW-Scale green hydrogen production,”*Int J Hydrogen Energy*, vol. 138, pp. 260–272, Jun. 2025, doi: 10.1016/j.ijhydene.2025.05.170.